

B1202 (Published elsewhere)

Redox Cycling of Ni/YSZ and Ni/GDC Anodes for Metal-Supported Fuel Cells

Florian Thaler (1), David Udomsilp (1), Wolfgang Schafbauer (2), Cornelia Bischof (2), Yosuke Fukuyama (3), Yohei Miura (3), Mari Kawabuchi (3), Shunsuke Taniguchi (4), Satoshi Takemiya (4), Alexander K. Opitz (5), Martin Bram (1)

(1) Forschungszentrum Jülich GmbH, Institute of Energy and Climate Research (IEK-1), D-52425 Jülich, Germany

(2) Plansee SE, Innovation Services, A-6600 Reutte, Austria

(3) Nissan Motor Co., Ltd. Nissan Research Center, 1, Natsushima, Yokosuka-shi, Kanagawa 237-8523, Japan

(4) Kyushu University, 744 Motooka Nishi-ku, Fukuoka 819-0395, Japan

(5) Vienna University of Technology, Institute of Chemical Technologies and Analytics A-1060 Vienna, Austria

Tel.: +49-2461-61-9706

f.thaler@fz-juelich.de

Abstract

Metal-supported fuel cells (MSCs) are promising candidates for non-stationary applications like auxiliary power units or range extenders in battery electric vehicles. They are attractive due to their potential to withstand fast thermal cycles and vibrations during cell operation. In addition, they have to withstand redox cycles, which might occur during start-up and shut-down of the fuel cell stack. Recently, a novel nickel/gadolinium doped ceria anode (Ni/GDC) was introduced in the metal-supported fuel cell concept of Plansee SE which almost tripled current density compared to the standard cell concept with a Ni/YSZ anode. In the present work, both cell concepts were compared regarding their ability to withstand harsh redox cycles. Therefore, after initial check at 750 °C, cell performance of button cells after controlled redox cycles was investigated at different temperature steps respectively. Re-oxidation temperature of the anodes was varied between 300 and 700 °C for 10 min in air. Afterwards, reduction of the anode was conducted by purging anode side with N₂ for 10 min and then going back to standard cell operation conditions with H₂ supply. The response of cell performance on redox cycling was recorded continuously. While standard MSCs with Ni/YSZ anode showed a strong degradation after a few cycles if the oxidation was conducted at temperatures above 600 °C, novel MSCs with Ni/GDC anode showed a remarkable resistance against re-oxidation. For a deeper understanding of this behavior, microstructural investigation of the Ni/GDC anode and the adjacent electrolyte was performed within the tested cells by FE-SEM and FIB-SEM 3D structure analysis. Furthermore, electrochemical behavior of Ni/GDC anode was investigated at a larger cycle number of up to 50 redox cycles with 2 h air supply each.

Introduction

In the framework of the “Christian Doppler Laboratory for Interfaces in Metal-Supported Electrochemical Energy Converters” (CD-Lab), investigative work on MSCs based on the Plansee concept from 2008 was carried out, concerning the improvement of electrochemical performance and the long term durability of the cells. The CD-Lab project was funded in 2014 as a close collaboration between academic members of Forschungszentrum Jülich GmbH, Vienna Technical University and the Austrian industrial partners Plansee SE and AVL List GmbH. Since two years, Nissan Motor Co. Ltd. and the Kyushu University in Japan are joining the consortium as associate partners. Within this cooperation electrochemical tests during reduction and re-oxidation (redox cycles) of the cells were performed at the “Next Generation Fuel Cell Center” (NEXT-FC) and Nissan. Also, microstructural changes were investigated via FIB-SEM and 3D-reconstruction. Both techniques were provided by the Kyushu University and Nissan.

1. Scientific Approach

Metal-supported fuel cells (MSCs) have some promising advantages over conventional ASCs, including a better thermal cyclability due to their well-adapted coefficient of thermal expansion (CTE) and lower heat capacity as well as lower material cost of the ferritic steel compared to conventional cermet (zirconia and nickel). In literature, state-of-the-art MSC concepts from different companies were reviewed regarding their requirements for manufacturing and their technology readiness level (TRL) [1, 2]. Thus, the Plansee concept is a third-generation solid oxide fuel cell (SOFC), very similar to an anode supported cell (ASC) with a cost efficient porous metallic support instead of the porous ceramic substrate. Fig. 1 illustrates the setup of the current Plansee MSC.

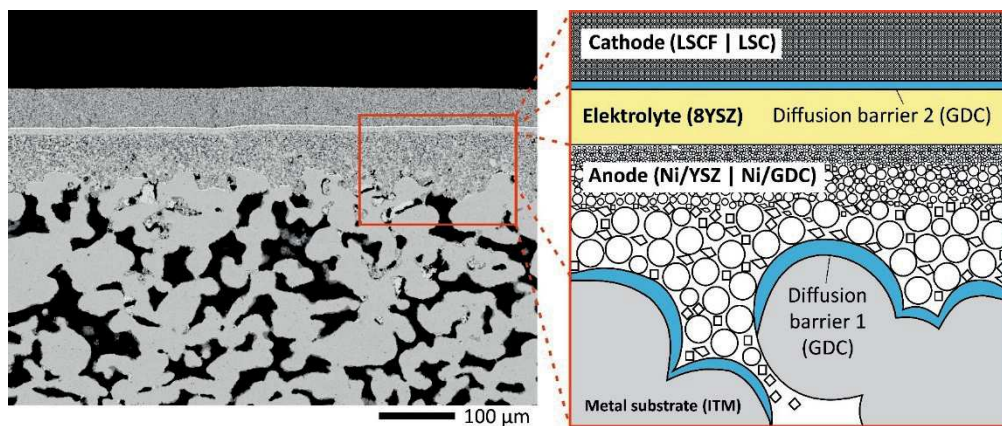


Fig. 1: General setup of the MSC developed by Plansee SE

Re-oxidation of metallic Ni in the state-of-the-art Ni/YSZ anode of ASCs leads to microstructural changes and volume expansion of up to 69 % and causes irreversible damage due to cracks in the electrolyte, as known from [2]. System-related or accidental re-oxidation of the anode typically occurs during start-up and shut down, which is performed more frequently for automotive use than for a stationary use of a SOFC stack. Therefore, redox tolerance is one of the essential criteria for good cell performance and long lifetime for auxiliary power unit (APU) or range extender (REx) application. The aim of this study was to investigate re-oxidation behavior of MSC anodes under real operation conditions to understand materials degradation and predict potential failure of the cells. MSCs have the potential to withstand harsh redox cycles without damage of the functional layers.

2. Experimental

Short description of MSC manufacturing:

The MSC cell design used in this work is related to the conventional state-of-the-art Plansee concept, consisting of a 0.8 mm thick porous metal support (Intermediate Temperature Metal, ITM), a 40 μm graded multilayer anode, a 4 μm dense electrolyte membrane (8YSZ) and a 40 μm LSCF cathode as top layer. To avoid interdiffusion, a 500 nm GDC DBL is applied on the ITM substrate and the electrolyte by magnetron sputtering. The anode is graded from coarse particles (1st layer) next to the metal substrate, to medium size in the interlayer (2nd layer) and very fine structure in the electrochemically active anode functional layer (3rd layer) in contact with the electrolyte. The ratio of Ni to YSZ particles was adjusted to 80:20 wt.-%, while the Ni:GDC ratio was reduced to 60:40 wt.-% due to coarsening of the Ni during sintering of the anode [4]. A more detailed description of the MSC manufacturing can be found in [5]. Button cells with a diameter of 29.5 mm are cut by laser cutting from larger rectangular half-cells. Subsequently, a cathode of 9 mm diameter is applied by screen printing.

Description of redox cycling and information about the testing equipment:

The redox cycling experiments in combination with the electrochemical testing as well as microstructural analysis were conducted at the "Next Generation Fuel Cell Center" (NEXT-FC, Kyushu University, Fukuoka, Japan) and Nissan. All tests were performed on button cells of 29.5 mm total diameter with an active cathode area of 0.64 cm² (\varnothing 9 mm) which are extracted from larger cells, as described before. For 10 min Redox testing between 300 and 700 °C, the cells were sandwiched between platinum meshes and the cramping force was added by test jig which was made of HastelloyTM metal. They were sealed by Thermiculite[®] compression seal to work in a wide temperature range. For 2 h Redox testing, the cells were placed between two alumina tubes and sealed with a commercial glass by heating the furnace to 850 °C under dual gas atmosphere. To ensure good electrical contacting of the cathode and anode, for both types of tests platinum meshes and wires were used. Porous alumina tips at the end of the tubes ensured a uniform gas distribution over the functional cathode and anode area.

After sealing at 850 °C, an initial performance check was performed by measuring the current-voltage characteristics (IV) and electrical impedance spectroscopy (EIS) at 750 °C under OCV conditions. Subsequently, the temperature was reduced to a temperature at which anode re-oxidation might occur under real operating conditions. Starting from 300 °C the anode gas was first switched to N₂ for 10 min to purge the lines, followed by 10 min oxidizing in air and another 10 min of purging with N₂ before the gas was switched back to H₂. This redox cycling procedure was repeated for 7 cycles at a particular temperature of 300 °C, 400 °C, 500 °C, 600 °C and 700 °C respectively. The electrochemical performance of the cells was measured after 7 cycles at each temperature. According to that, each tested cell has been subjected to a total of 35 redox cycles in a temperature range of 300-700 °C. *Fig. 2* schematically illustrates the performed testing procedure.

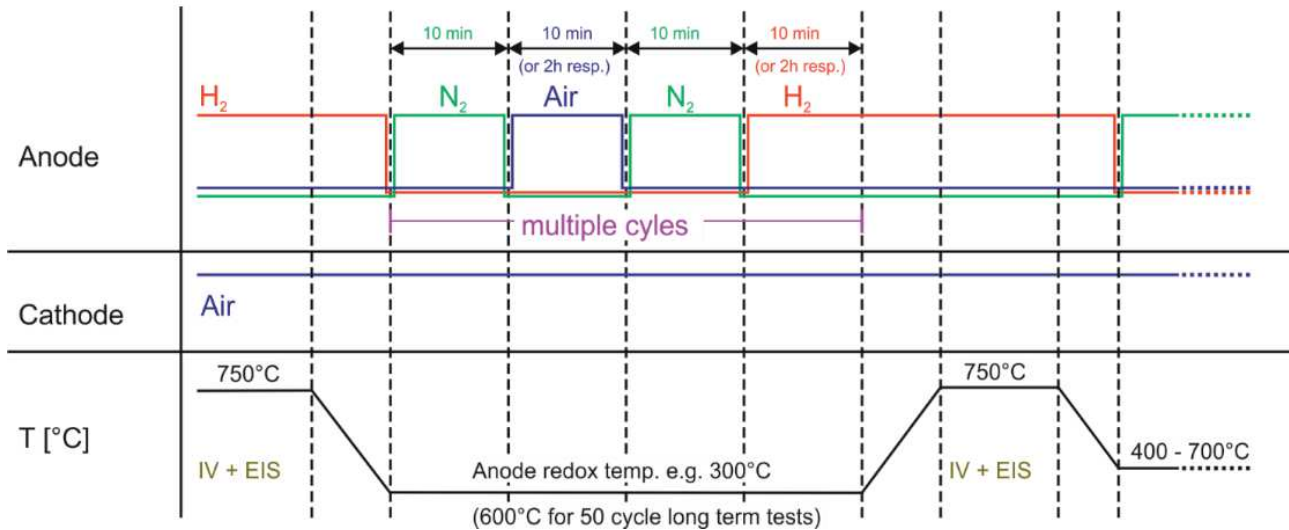


Fig. 2: Schematic of the redox cycling experiment for a particular re-oxidation temperature of 300 °C.

Additionally, a long term test was performed on a cell with Ni/GDC anode. 50 redox cycles were performed at 600 °C with 2 h oxidation and 2 h reduction time for each particular cycle. In this test, the performance check between the cycles was done at 600 °C as well.

Details about FIB-SEM with 3D structural analysis:

For acquisition of the structural information of the tested samples a FEI (Thermo Fischer Scientific) dual beam Helios NanoLab600i[®] of the NEXT-FC at Kyushu University was used. Therein a Focused Ion Beam (FIB) is combined with a Scanning Electron Microscope (SEM) to provide detailed insights in the spatial texture of the porous anode structure. The FIB unit periodically detaches thin layers from the sample surface which in meanwhile is recorded layer by layer with the SEM. As a result, the individual pictures can be combined to a three-dimensional image of the probed sample volume. By means of digital image processing, each phase can be separated on the basis of differing grey values in the SEM images. Thus, volume fractions and positions of the ceramic and nickel particles as well as the pores can be calculated. Furthermore, the tortuosity of the particles and pores, the distribution and density of triple phase boundaries (TPBs) and the interface area of each phase can be obtained from this data.

3. Results

Electrochemical performance of the cells after redox testing:

After each 7 redox cycles at a particular temperature, electrochemical performance check of the cells was performed by measuring IV curves and EIS spectra at 750 °C, as described above. The results in Fig. 3 show that current density decreases drastically after the re-oxidation of Ni/YSZ anode at 600 °C and above. Re-oxidation at 300-500 °C did not induce cell degradation compared to the reference performance before redox cycling (beginning of life, BOL). The cell with Ni/GDC anode exhibits an improved redox tolerance and no degradation in cell performance after the re-oxidation in the full temperature range of 300-700 °C. It should be also noted that the measured current density of the cells with Ni/GDC anode is about three times higher than for the standard Ni/YSZ anode. For

instance, initial current density of the cell with Ni/GDC anode was about 2.7 A/cm² at a voltage of 0.7 V in comparison to 0.9 A/cm² for the Ni/YSZ anode.

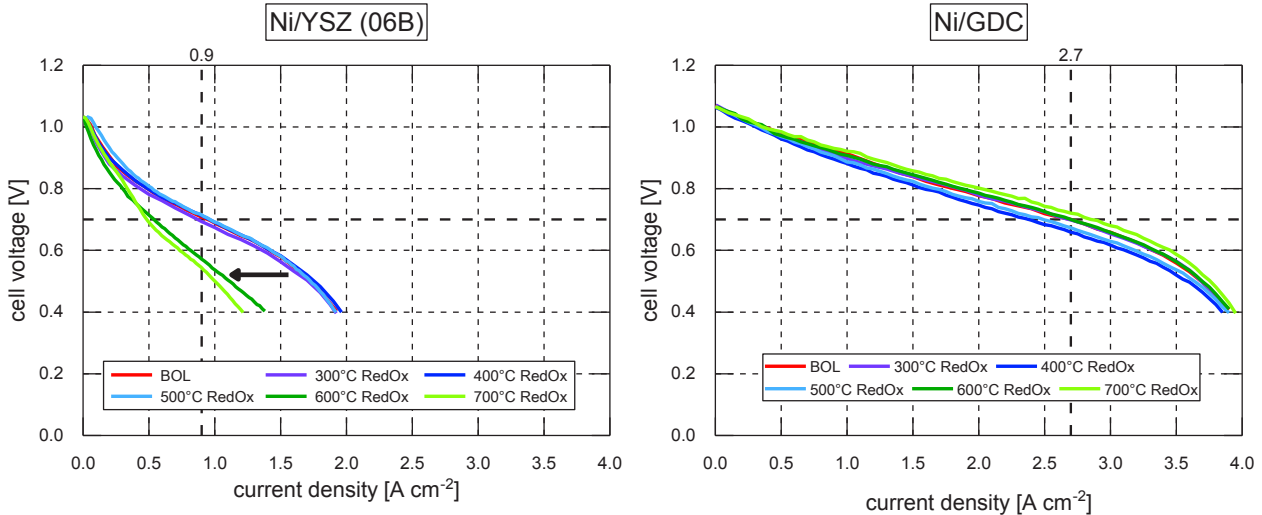


Fig. 3: Performance check (IV at 750 °C) of cells with Ni/YSZ (06B) and Ni/GDC anode after 7 re-oxidation cycles at particular temperatures of 300-700 °C.

Electrochemical impedance spectroscopy was conducted after each set of particular redox cycles. Especially, ohmic resistance of the Ni/YSZ standard cells after 600 °C and 700 °C re-oxidation increased from 0.12 to 0.3 Ω cm². For the Ni/GDC anode no increase in ohmic resistance was recorded, regardless of the redox temperature according to Fig. 4.

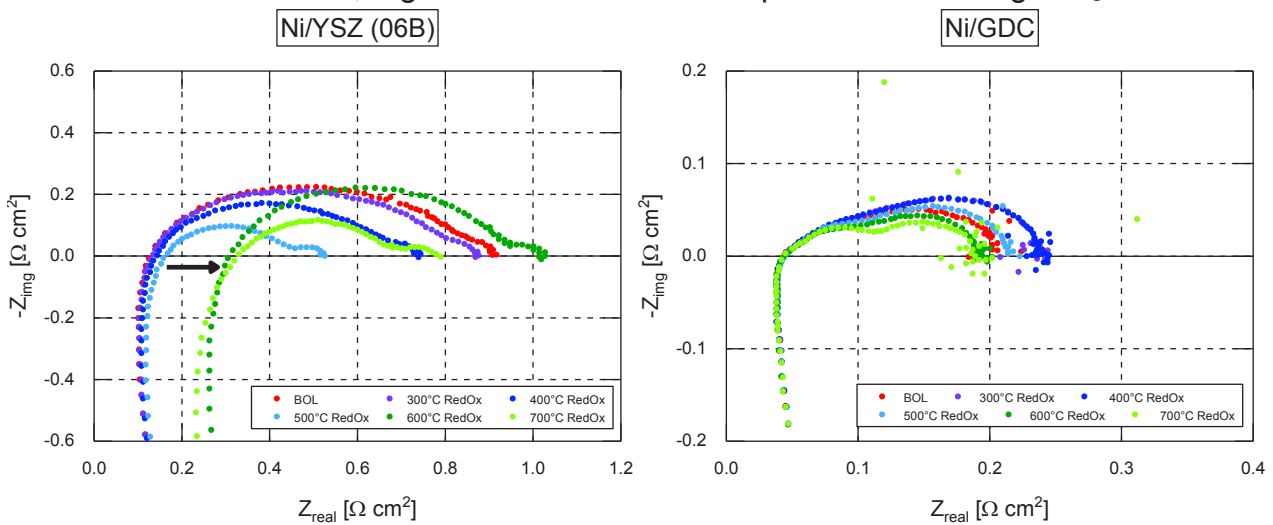


Fig. 4: Electrochemical impedance spectroscopy (EIS) of the cells with Ni/YSZ (left) and Ni/GDC (right) anode after re-oxidation at particular temperatures of 300 – 700 °C.

After the cycling test the electrolyte of the Ni/YSZ sample was partially peeled off from the anode side, while the cell with Ni/GDC anode did not show delamination. This might be the reason for the increase of ohmic resistance in the Ni/YSZ cell after the re-oxidation at 600 °C.

The preliminary experiments with a total of 35 short redox cycles at different re-oxidation temperatures between 300-700 °C revealed a significantly higher redox tolerance of the cells with Ni/GDC anode compared to cells with Ni/YSZ anode, even at elevated redox temperatures of 600-700 °C. For this reason longer redox cycling tests with a higher number of cycles were performed on Ni/GDC anodes, as described before.

Long-term durability of new Ni/GDC anode:

Electrochemical performance of a cell during 50 cycles of re-oxidation at 600 °C was investigated. The graph in Fig. 5 shows the beginning of cell degradation after more than 20 redox cycles. With increasing number of redox cycles, the ohmic resistance increases and cell performance decreases simultaneously. The strong increase in ohmic resistance at the end of the redox test can be attributed to a delamination of the electrolyte from the anode as can be seen from the SEM images of the tested cells.

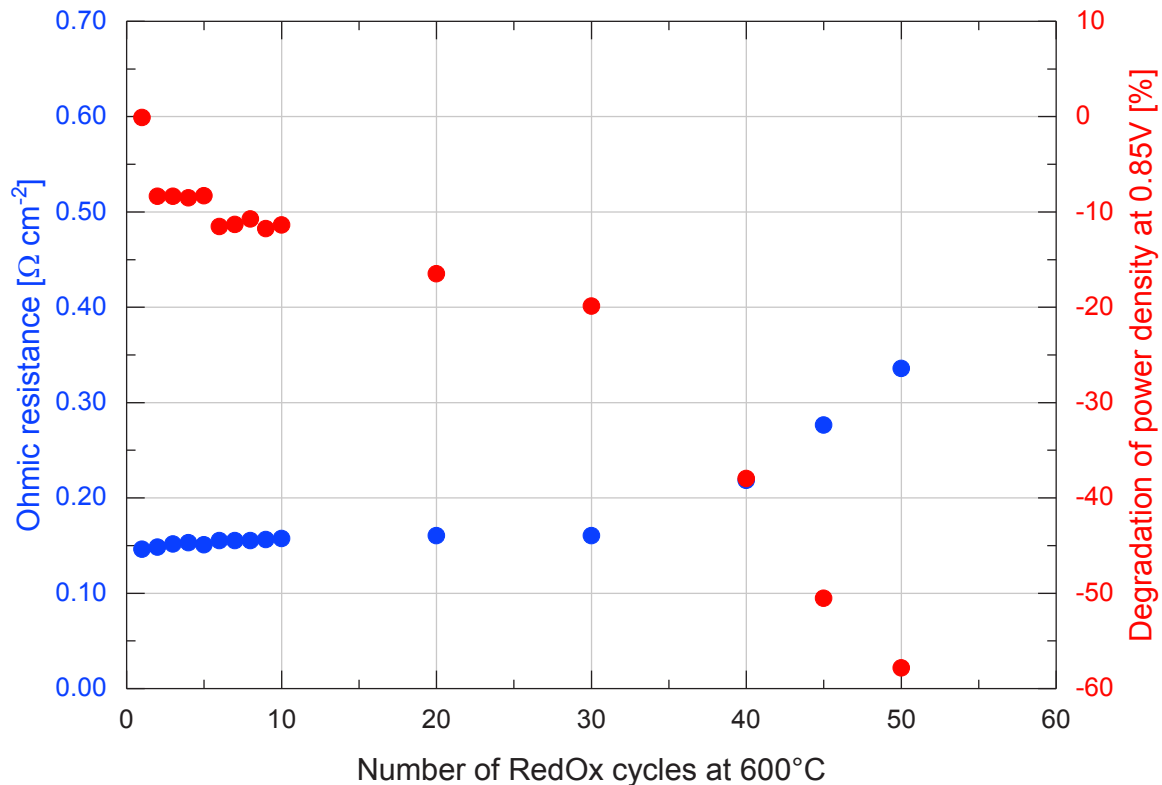


Fig. 5: Degradation in power density of a MSC with 3rd layer Ni/GDC anode as a result of the increasing ohmic resistance with number of redox cycles at 600 °C.

Microstructural change in 3rd layer of the anode due to redox cycling:

The microstructure of the anodes before and after multiple cycle re-oxidation (according to Fig. 2) was analyzed by FIB-SEM and 3D-reconstruction technique. Fig. 6 shows the microstructure of the anode's 2nd and 3rd layer before and after the 35 short redox cycles at temperatures between 300-700 °C. After redox cycling, the Ni structure was changed from spherical grains to a porous microstructure, both in Ni/YSZ and Ni/GDC anode's functional 3rd layer. Also in the 2nd layer which contains Ni/YSZ for both cell types, a strong microstructural change occurred during the test. However, within the Ni/GDC 3rd layer the change of the Ni-phase is less pronounced than in Ni/YSZ 3rd layer anode.

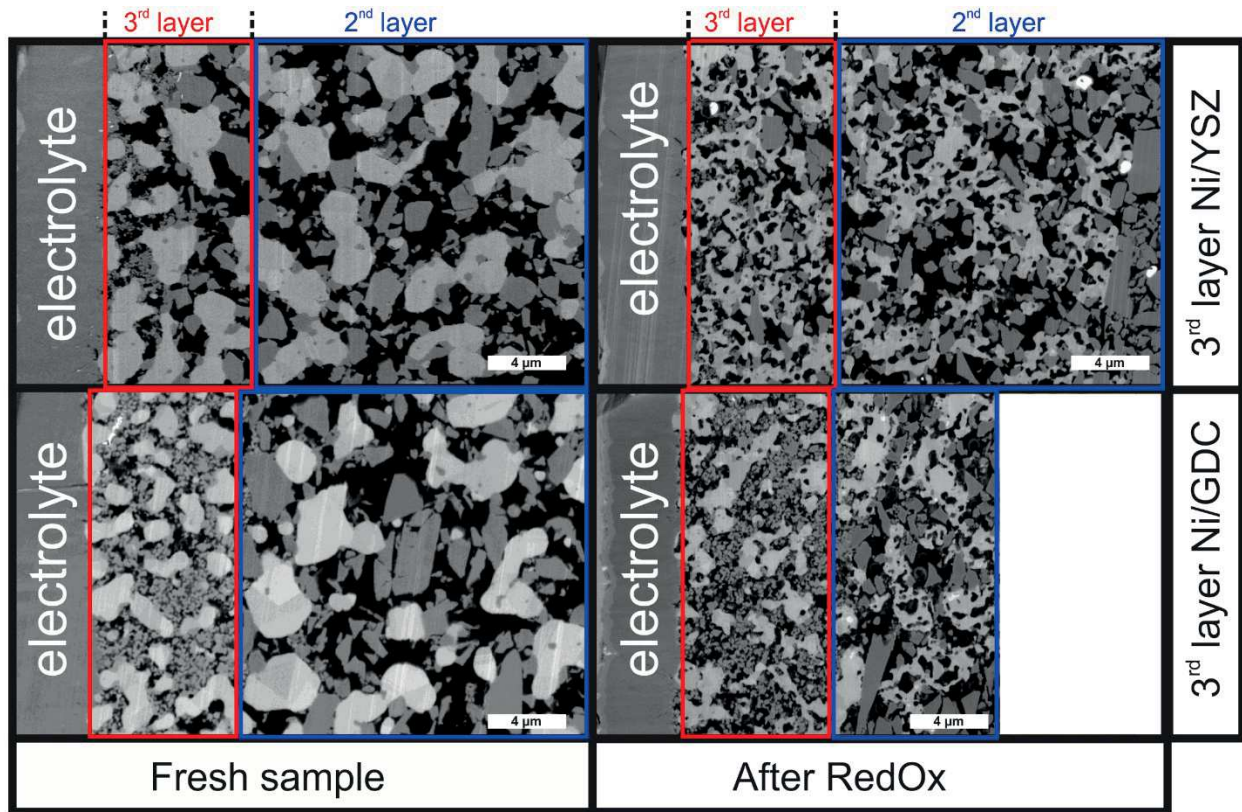


Fig. 6: SEM micrographs from FIB-SEM of the 2nd and 3rd layer of the anode before and after 35 redox cycles at 300-700 °C with 10 min re-oxidation at each cycle according to Fig. 2.

By the use of FIB-SEM technique, a three-dimensional imaging of the microstructure was reconstructed from the single layer SEM images. From the reconstructed 3D microstructure, information about pore and particle size distribution was extracted as represented in Fig. 7. It can be seen from this data, that Ni and YSZ particles as well as pore size was drastically reduced in the tested sample after redox cycling test in the 3rd layer Ni/YSZ anode. SEM and reconstructed 3D images indicate that the Ni particle structure was changed from spherical to a porous doughnut shaped structure, which also has an influence on the calculated particle size. The sphere packing algorithm has to be adapted for the new microstructure. Within the Ni/GDC anode, only particle size of the Ni was reduced from 0.63 μm to 0.33 μm after the redox testing.

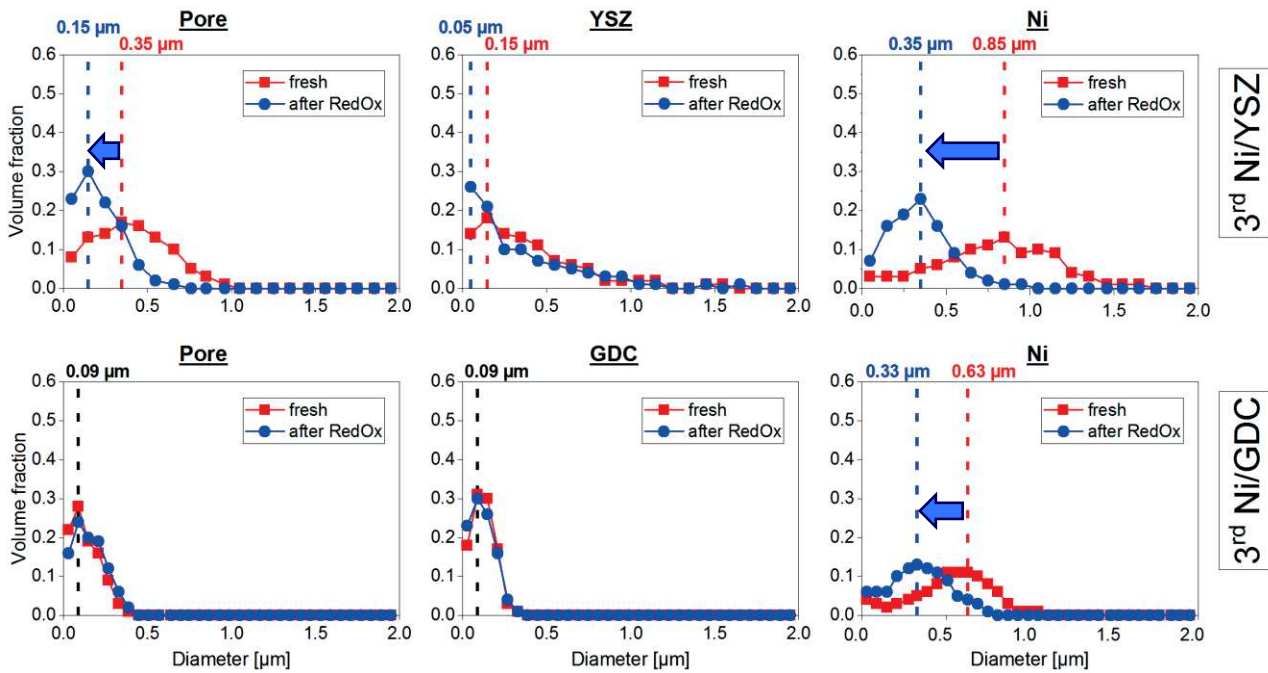


Fig. 7: Reconstructed information about pore and particle size distribution of 3rd layer Ni/YSZ and 3rd layer Ni/GDC anodes before and after 35 redox cycles at 300-700 °C.

FIB-SEM 3D reconstruction technique also allows us to calculate the interface area between pores and YSZ (or GDC resp.), YSZ (GDC) and Ni particles and between Ni and the pores. As listed in *Tbl. 1*, mostly the Ni-pore and the YSZ-Ni interface area increased in the tested Ni/YSZ sample which can be explained by the change in the microstructure of the Ni-particles. According to these results Ni/GDC anode remained unaffected for the most part, only the pore-GDC interface area slightly increased. These data do not clearly match the impression from the SEM image in *Fig. 6*, where the microstructure of Ni particles in the tested Ni/GDC 3rd layer also changed to become porous. For this reason, the Ni-pore interface should clearly increase in the Ni/GDC anode as well. A reason for this mismatch could be the unclear identification of the newly generated pores within the Ni particles by 3D reconstruction method. Optimization of the corresponding analyzing algorithms is required.

Tbl. 1: Calculated surface area of pore-YSZ (pore-GDC), YSZ-Ni (GDC-Ni) and Ni-pore interfaces in 3rd layer Ni/YSZ and 3rd layer Ni/GDC anodes before and after redox cycling test at 300-700 °C.

	3 rd layer Ni/YSZ		3 rd layer Ni/GDC		
	Fresh sample	After redox (300-700 °C)	Fresh sample	After redox (300-700 °C)	
Pore-YSZ	3.20	3.71	Pore-GDC	7.72	8.55
YSZ-Ni	1.69	2.33	GDC-Ni	3.63	3.77
Ni-Pore	0.35	2.04	Ni-Pore	0.75	0.86

According to the microstructural change in the 3rd layer Ni/GDC anode tested at 600 °C for multiple redox cycles of 2 hours each, FIB-SEM with 3D reconstruction analysis indicated no significant change in anode microstructure after 5 redox cycles. After 50 cycles the calculated GDC content apparently increased around 15 % at the expense of Ni in the 3rd layer as seen from *Fig. 8*. The fresh sample has a well-defined distribution of spherical Ni and fine GDC particles, which can be clearly separated from the pores. However, after 50 redox cycles at 600 °C the boundary between Ni and pore phase became unclear despite the high resolution of the SEM images. A possible reason for the unclear borders is that Ni

metal might have changed to alloy or was covered by Fe or Cr in some area and for this reason the gray value of the Ni phase changed in the image. As a result, differentiation between Ni and pore at the Ni-pore interface became indistinct which caused an incorrect GDC-Ni ratio. Furthermore, the delamination of the electrolyte is also illustrated in the SEM image after 50 redox cycles in Fig. 8.

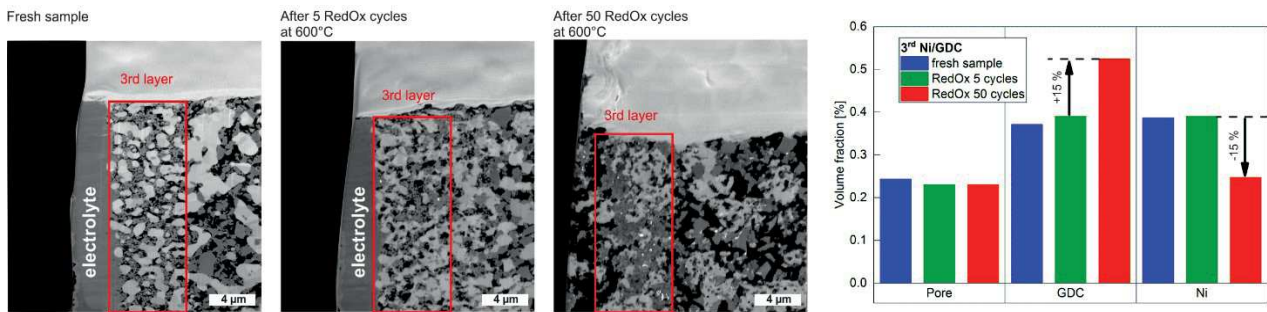


Fig. 8: FIB-SEM images and reconstructed volume fraction of 3rd layer Ni/GDC anode after 5 and 50 redox cycles at 600 °C for 2 hours anode re-oxidation per cycle.

Conclusions

In the present work, redox cycling experiments on MSCs with conventional 3rd layer Ni/YSZ and novel 3rd layer Ni/GDC anodes were introduced. It could be shown that Ni/GDC offers a higher redox tolerance than Ni/YSZ even up to 700 °C. The high current density of about 2.7 A/cm² at 0.7 V and 750 °C for the cell with Ni/GDC anode remained constant over several short redox cycles (10 min re-oxidation) at temperatures between 300-700 °C. On the other hand, initial current density of 0.9 A/cm² of a cell with the Ni/YSZ standard anode dropped to less than 0.5 A/cm² together with an increased ohmic resistance after redox cycling at 600-700 °C. The degradation was explained by the partial delamination of the electrolyte from the anode side of the Ni/YSZ cell after the test. To confirm the long term durability of the Ni/GDC 3rd layer of the anode, multiple redox cycles at 600 °C were performed with 2 hours of re-oxidation and 2 hours of reduction per cycle. Cell performance remained largely unchanged until a number 20 redox cycles. Beyond that, a strong decrease in power density of almost 60 %, accompanied by an increasing ohmic resistance was observed during cycling for up to 50 redox cycles. Microstructural investigations of the 3rd layer of Ni/YSZ and Ni/GDC anode indicated a stronger degradation of the Ni/YSZ microstructure than the novel Ni/GDC anode. However, also the Ni/GDC anode clearly degraded after multiple cycles at 600 °C and electrolyte delamination was observed after the test with 50 redox cycles. At least the Ni particles changed from spherical to a finer porous structure with less percolation between the individual grains, both in the 3rd layer Ni/GDC anode as well as in the Ni/YSZ 2nd layer. 3D reconstruction technique by FIB-SEM indicated extensive changes in Ni/YSZ microstructure, but also in the 3rd layer Ni/GDC anode after the long-term cycles.

Acknowledgements

Christian Doppler Laboratories are funded in equal shares by the public authorities and the companies directly involved in the laboratories. The most important funding source of the public authorities is the Austrian Bundesministerium für Wissenschaft, Forschung und Wirtschaft (BMWFW). The funding is highly acknowledged by the authors. Moreover, the authors would like to thank the industrial project partners Plansee SE and AVL List GmbH as well as the associate partners Nissan Motor Co., Ltd. and Kyushu University in Fukuoka, Japan.



References

- [1] Krishnan, V. V. (2017). "Recent developments in metal-supported solid oxide fuel cells." Wiley Interdisciplinary Reviews: Energy and Environment, e246. DOI: 10.1002/wene.246.
- [2] Tucker, M. C. (2010). "Progress in metal-supported solid oxide fuel cells: A review." Journal of Power Sources 195(15): 4570-4582.
- [3] Ettler, M., H. Timmermann, J. Malzbender, A. Weber and N. H. Menzler (2010). "Durability of Ni anodes during reoxidation cycles." Journal of Power Sources 195(17): 5452-5467.
- [4] Rojek-Wöckner, V. A., A. K. Opitz, M. Brandner, J. Mathé and M. Bram (2016). "A novel Ni/ceria-based anode for metal-supported solid oxide fuel cells." Journal of Power Sources 328: 65-74.
- [5] Roehrens, D., U. Packbier, Q. Fang, L. Blum, D. Sebold, M. Bram and N. Menzler (2016). "Operation of Thin-Film Electrolyte Metal-Supported Solid Oxide Fuel Cells in Lightweight and Stationary Stacks: Material and Microstructural Aspects." Materials 9(9): 762.

*Remark: Only the abstract is officially available, because the authors publish elsewhere.
Please see Presentations on www.EFCF.com/LIB or contact the authors directly.*